To appear in August 1996 Astronomical Journal

The FIRST Bright QSO Survey

Michael D. Gregg
Institute for Geophysics and Planetary Physics
Lawrence Livermore National Laboratory
gregg@igpp.llnl.gov

Robert H. Becker
University of California at Davis
and
Institute for Geophysics and Planetary Physics
Lawrence Livermore National Laboratory
bob@igpp.llnl.gov

Richard L. White
Space Telescope Science Institute
rlw@stsci.edu

David J. Helfand[1]
Columbia Astrophysics Laboratory
djh@carmen.phys.columbia.edu

Richard G. McMahon
Institute of Astronomy, Cambridge
rgm@ast.cam.ac.uk

Isobel M. Hook
University of California at Berkeley
imh@bigz.berkeley.edu

ABSTRACT

The FIRST radio survey provides a new resource for constructing a large quasar sample. With source positions accurate to better than $1''$ and a point source sensitivity limit of 1 mJy, it reaches 50 times deeper than previous radio catalogs. We report here on the results of the pilot phase for a FIRST Bright Quasar Survey (FBQS). Based on matching the radio catalog from the initial 300 deg^2 of FIRST coverage with the

[1]Visiting Astronomer, Kitt Peak National Observatory, National Optical Astronomy Observatory

optical catalog from the Automated Plate Machine (APM) digitization of Palomar Sky Survey plates, we have defined a sample of 219 quasar candidates brighter than E = 17.50. We have obtained optical spectroscopy for 151 of these and classified 25 others from the literature, yielding 69 quasars or Seyfert 1 galaxies, of which 51 are new identifications. The brightest new quasar has an E magnitude of 14.6 and z = 0.91; four others are brighter than E = 16. The redshifts range from z=0.12 to 3.42. Half of the detected objects are radio quiet with $L_{21cm} < 10^{32.5}$ ergs/s. We use the results of this pilot survey to establish criteria for the FBQS that will produce a quasar search program which will be 70% efficient and 95% complete to a 21-cm flux density limit of 1.0 mJy.

Subject headings: quasars: radio selected — quasars: luminosity function

1. Introduction

The number of QSOs has ballooned over the past decade, largely as a result of systematic large-area surveys. The majority of these surveys have been based on optical selection criteria, such as the Large Bright Quasar Survey (LBQS; Hewett, Foltz, & Chaffee 1995) and the Edinburgh Quasar Survey (Goldschmidt et al. 1992), in marked contrast to the earliest radio-selected QSO searches. The recent emphasis on optically-selected samples is due in part to their higher efficiency; previous radio selected samples suffer mainly from the difficulty of identifying optical counterparts from poor radio positions. Additionally, past radio selected samples have been largely insensitive to radio quiet objects, which make up the preponderance of the QSO population. Yet optically selected quasar samples have their own disadvantages, possibly excluding QSOs with unusual colors. For example, it has recently been suggested that there is a large population of 'dusty' QSOs which has been missed by recent QSO surveys (Webster et al. 1994). A radio selected sample can, in principle, be immune to optical color selection effects.

We show here that the NRAO[2] Very Large Array (VLA) FIRST[3] survey (Becker, White and Helfand 1995; hereafter BWH) is capable of generating a radio selected sample of quasars which can achieve the very high efficiency of optical surveys. Such a new complete sample of radio-selected QSOs will help address several unresolved questions, such as the surface density of bright quasars and whether or not there is differential evolution between radio loud and radio quiet QSOs.

We present the results of the pilot phase of the FIRST Bright Quasar Survey (FBQS) based

[2]The National Radio Astronomy Observatory is operated by Associated Universities, Inc., under cooperative agreement with the National Science Foundation

[3]The FIRST Survey World Wide Web homepage is http://sundog.stsci.edu

on the initial 300 deg^2 imaged by the VLA FIRST survey in 1993. The early results, especially some of the more unusual quasars in the sample, may be of particular interest to others. In § II we discuss the selection of candidate QSOs based on a comparison of the FIRST survey catalog of radio sources with the Automated Plate Machine (APM) catalog of POSS I objects (McMahon & Irwin 1992). In § III, we describe the optical observations used to confirm sources as QSOs and present the spectroscopic results. We then discuss the efficiency of the survey in § IV, concluding in § V with a discussion of future plans for the survey.

2. Selection of QSO Candidates

The preliminary VLA FIRST catalog of radio sources covered 306 deg^2 in a narrow strip through the north Galactic pole (BWH) and contained $\sim 27,000$ sources, complete to a flux density limit of 1 mJy for point sources. Comparisons between the FIRST catalog and standard radio calibration sources indicate that the systematic astrometry errors are $< 0\farcs2$ in both RA and Dec. Extensive tests also indicate that even for the faintest radio sources, positions are accurate to $\pm 1''$ (90% confidence). Nonetheless, in matching to optical counterparts we required only $2''$ agreement in position, in part to allow an independent check on the radio positional accuracy (see section IV).

QSO candidates were selected by matching FIRST survey sources to the APM catalog of the Palomar Observatory Sky Survey (POSS I). Objects classified by the APM as stellar on either of the two POSS I emulsions, O (blue) or E (red), brighter than 17.5 magnitude on the E plate, and within $2''$ of a FIRST radio source were included in this pilot quasar survey. In keeping with the desire to avoid optical selection effects, no color cut was imposed on this initial candidate list.

The original National Geographic-Palomar Observatory Sky Survey was carried out using Eastman 103a-O and 103a-E emulsions. Plots of the effective system response for each are given in Minkowski & Abell (1963). The "O" and "E" passbands have effective wavelengths of roughly 4200Å and 6400Å, and effective widths of approximately 1200Å and 400Å, respectively. Except for the narrowness of the E passband, these are similar to Johnson B and Cousins R; the color transformation for normal stars is (B-R) = 0.875(O-E) + 0.073 (Bessell 1996, private communication). In what follows, we have chosen not to transform the magnitudes from O and E to a more standard system for two reasons. Objects with emission lines will not transform in a straightforward manner as do stars. Also, the errors in O and E are rather large. In a comparison of 33 QSOs for which the Automated Plate Scanner (http://isis.spa.umn.edu) magnitudes were available on-line, we obtain a scatter of 0.4 magnitudes in both O and E and 0.35 magnitudes in O-E. Much of the scatter can perhaps be attributed to the lack of field-by-field calibration of the APM catalog. Within this error range, O and E can be considered approximately equal to B and R magnitudes over the color range of our sample. We have begun an observing program at Lick Observatory to improve the optical photometry of the QSOs in the sample, however, the completeness of the survey remains problematic because of the large errors. We will address this issue in more detail in future installments of this survey.

The other selection criteria also raise some issues regarding completeness. The requirement of a $2''$ positional coincidence discriminates against QSOs associated with extended radio sources (lobes), selecting only those QSOs with nuclear radio emission or compact morphology as seen by the FIRST survey. Additional QSOs might be found by relaxing the coincidence requirements but only at the expense of additional chance coincidences. Part of the intent of the pilot survey is to explore the level of completeness arising from the morphological considerations.

With the above criteria, 219 QSO candidates were selected, 0.8% of the total FIRST catalog. Ninety-seven were classified as stellar on both POSS I emulsions. Another 29 were classified as stellar on the E plates only and 93 as stellar on the O plates only. Since the O magnitudes are often much fainter than the E magnitudes, their classification is typically less reliable, especially near the plate limit where the tendency is for the APM to classify these objects as stellar. This leads to a large number of apparently normal, red galaxies being included in the candidate list.

Using the NASA Extragalactic Database (NED), 25 of the 219 candidates were found to be already identified in the literature as QSOs or galaxies, leaving 194 objects for spectroscopic follow-up.

3. Optical Observations

The spectroscopy was carried out at Lick Observatory, Kitt Peak National Observatory, [4] and La Palma. The observations at Lick Observatory were made on the Shane 3-m telescope with the Kast spectrograph spanning the wavelength range 3500-8000Å. The Kitt Peak spectra are from the 4-m telescope with somewhat redder wavelength coverage (4500-9000Å) and have some overlap of second order at the red end. The La Palma 2.5-m telescope spectra span 5000 - 8000Å. All the spectra have a resolution of $\sim$ 5Å. Integration times were typically 10-15 minutes. Observing conditions varied markedly both in transparency and seeing. Sample QSO spectra are shown in Figure 1, including the brightest new quasar, BQ 0751+2919 with E magnitude = 14.6, and the highest redshift new quasar, BQ 0933+2845 with z = 3.42.

To date we have obtained optical spectra for 151 of the 194 previously unclassified QSO candidates. Because of the large range in brightness, the spectra vary in quality from signal-to-noise of 50 to $\sim$ 5. We have classified objects into five categories. Spectra with broad emission lines with $\sigma \gtrsim 1000$ kms^{-1}, much greater than typical galaxy velocity dispersions, are classified as QSOs. This classification draws no distinction between bona fide QSOs and Seyfert 1 galaxies; better optical images are required for this refinement, although the optical luminosities can be used to make a rough separation between the two (see below). Featureless spectra are designated as BL

---

[4] Kitt Peak National Observatory, NOAO, is operated by the Association of Universities for Research in Astronomy, Inc. (AURA), under cooperative agreement with the National Science Foundation

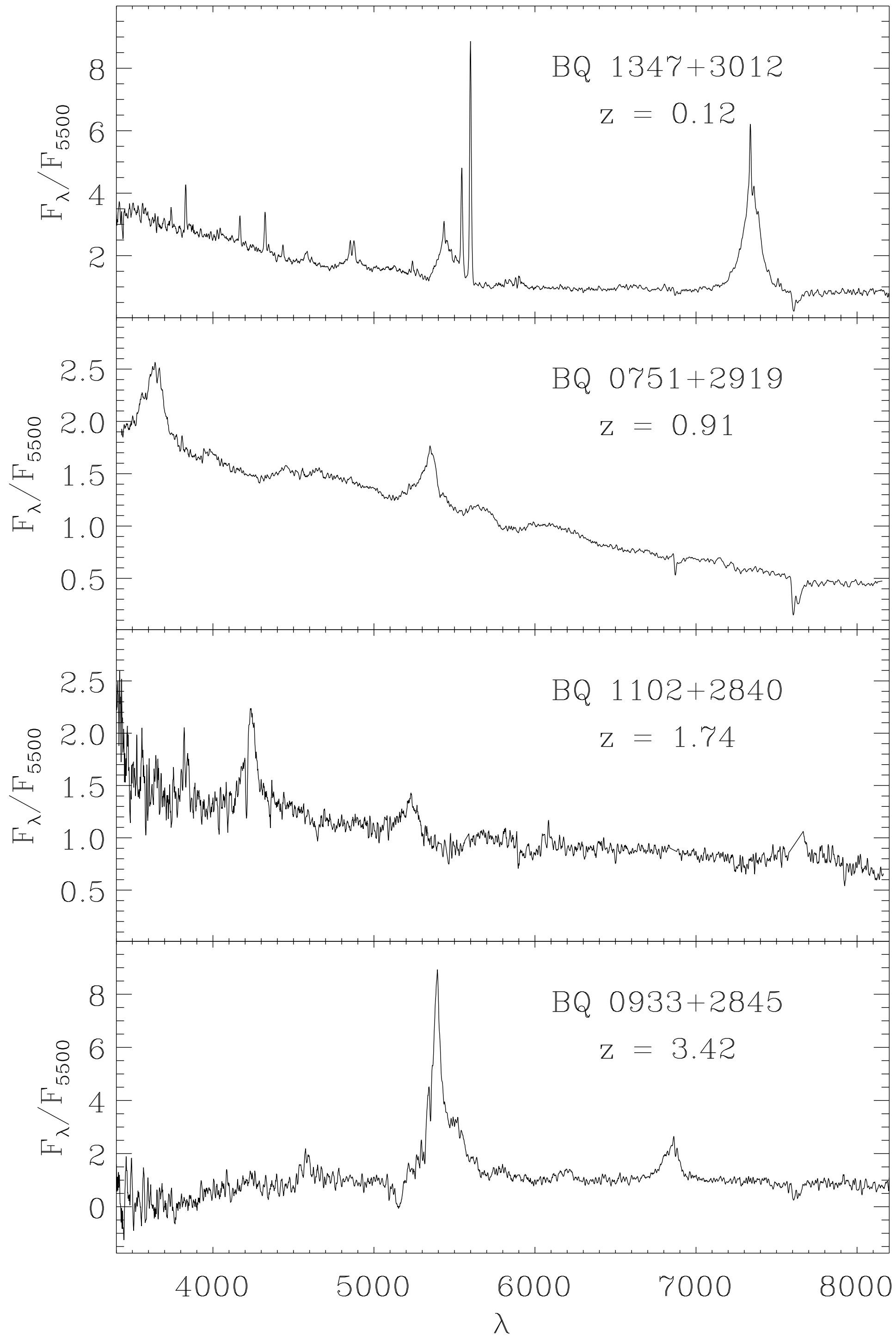

Fig. 1.— Sample optical spectra from the Lick Observatory Kast Double Spectrograph. BQ 0751+2919 is the brightest of the new quasars, with E = 14.6; BQ 0933+2845 is the highest redshift new quasar, with z=3.42.

Lacs. Spectra with narrow emission lines, $\sigma \sim 150 - 300$ kms^{-1}, are classed as ELG, making no distinction among true AGN, starburst, and ordinary star forming galaxies. The two remaining categories are galaxies with absorption lines only (ALG), and Galactic stars. All but 4 of the spectra provided positive classifications; these remaining 4 are among the lowest S/N spectra but are good enough to confidently rule out the presence of strong emission lines. On the basis of the radio association and a relatively red optical spectral energy distribution, we tentatively classify these 4 as ALGs, though the possibility exists that they are red Bl Lacs. The classifications of the 151 spectra and 25 NED-identified objects break down as 69 QSOs, 3 BL Lacs, 32 ELG, 41 ALG, and 31 stars. Despite the bright magnitude limit, only 15 of the QSOs were previously cataloged.

For each of the 69 QSOs found in the pilot survey region of 306 deg^2, Table 1 lists RA and Dec (J2000), O and E apparent magnitudes from the APM catalog, 20 cm flux density (S_{21}) for the nuclear radio source, total 20 cm flux density including radio lobes (for objects with multiple components), emission line redshift, the logarithm of the inferred radio luminosity for the nuclear radio source, and the absolute E magnitude. For consistency with other studies, we adopt $H_o = 50$ km s^{-1}Mpc^{-1} and $q_o = 0.5$ to compute the distance-dependent quantities using the relations from Weedman (1986). We assume that the spectral energy distributions are described by a simple power law in frequency with an exponent of $\alpha_R = -0.5$. Notes to Table 1 describe the radio morphology where it differs from a single compact component. Eleven of the QSOs have extended emission on a scale $> 10''$ while another five objects have measured single component sizes $> 2''.5$, the resolution limit of the FIRST Survey (White et al. 1996).

In Tables 2 and 3, we list similar data for the narrow emission line galaxies and the absorption line galaxies respectively. Data for the Galactic stars are contained in Table 4. Many, but not all, of the stars are chance coincidences (Becker et al. 1995).

Figure 2 shows the distribution of observed nuclear radio flux for the QSOs; every QSO in the sample with $S_{21cm} > 195$ mJy has been previously identified, an indication of the completeness threshold of previous radio-selected samples.

About 50% of the QSOs in the sample are radio quiet with $L_{21cm} < 10^{32.5}$erg s^{-1} Hz^{-1}, using a simple luminosity cut as the criterion for radio loudness (Schneider et al. 1992). With a flux density limit of 1 mJy, some radio quiet QSOs will be detectable in the FIRST survey out to a redshift of ~ 2. A histogram of the radio luminosities (Figure 3) has a suggestion of a deficit at $L_{21cm} \approx 10^{33}$erg s^{-1} Hz^{-1}, hinting at a bimodal distribution, roughly consistent with radio loud and radio quiet objects. As the survey progresses and the sample grows, the reality of the bimodality will be resolved, though it is already apparent that there is considerable overlap in the distributions. The narrow emission line galaxy (ELG) and absorption line galaxy (ALG) luminosities are shown for comparison (dashed line). The latter two classes have indistinguishable distributions.

Figure 4 displays a histogram of the redshift distribution for the 69 QSOs. The radio loud QSOs have been shaded to illustrate clearly the bias against detecting high redshift radio quiet

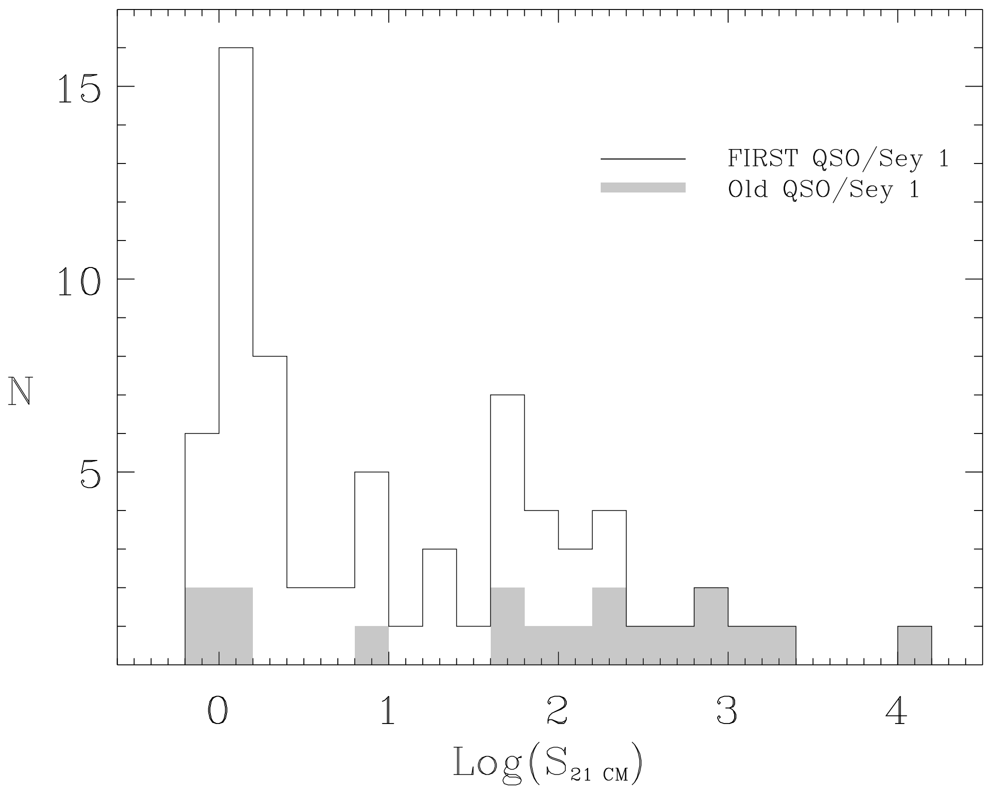

Fig. 2.— Distribution of observed nuclear 21 cm flux for the QSO sample. Previously known QSOs are shaded.

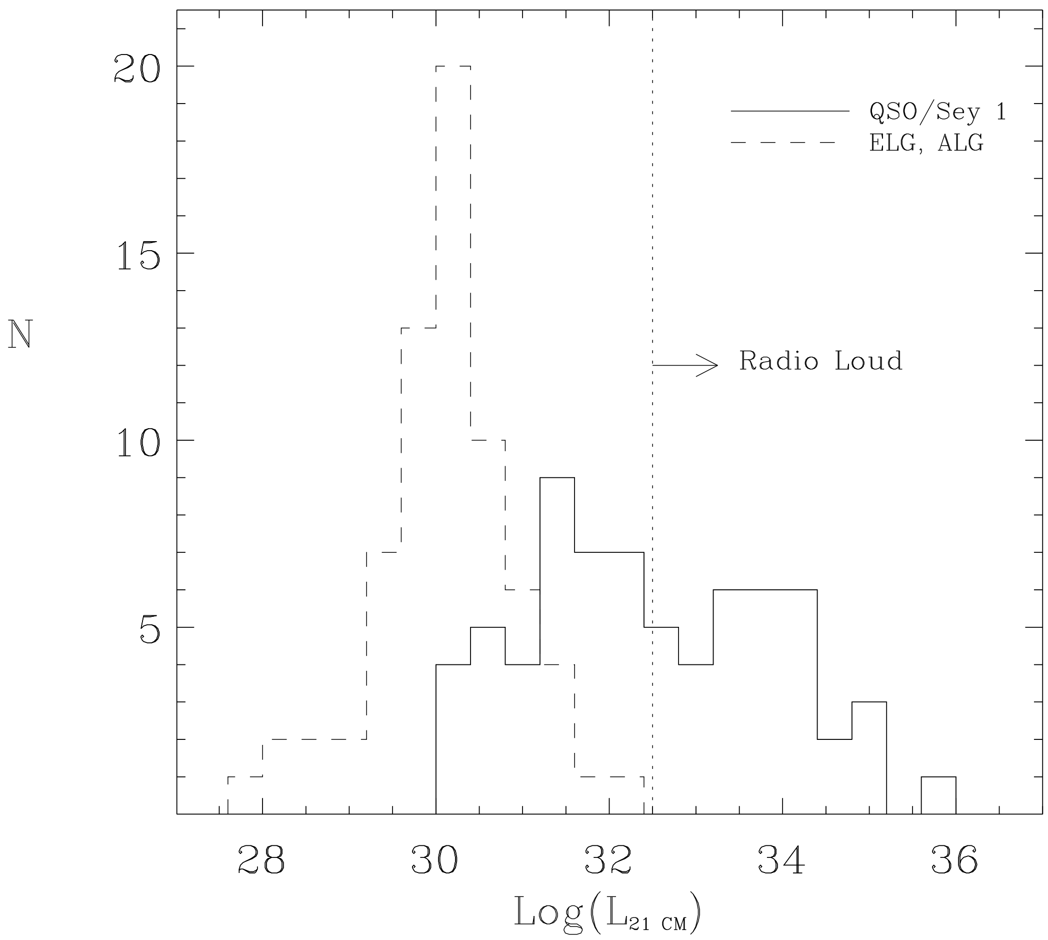

Fig. 3.— Histogram of the QSO/Seyfert 1 nuclear radio luminosities; there is a suggestion of a bimodal distribution between radio loud and radio quiet. The distribution of narrow emission line and absorption line galaxy radio luminosities (dashed histogram) is plotted for comparison.

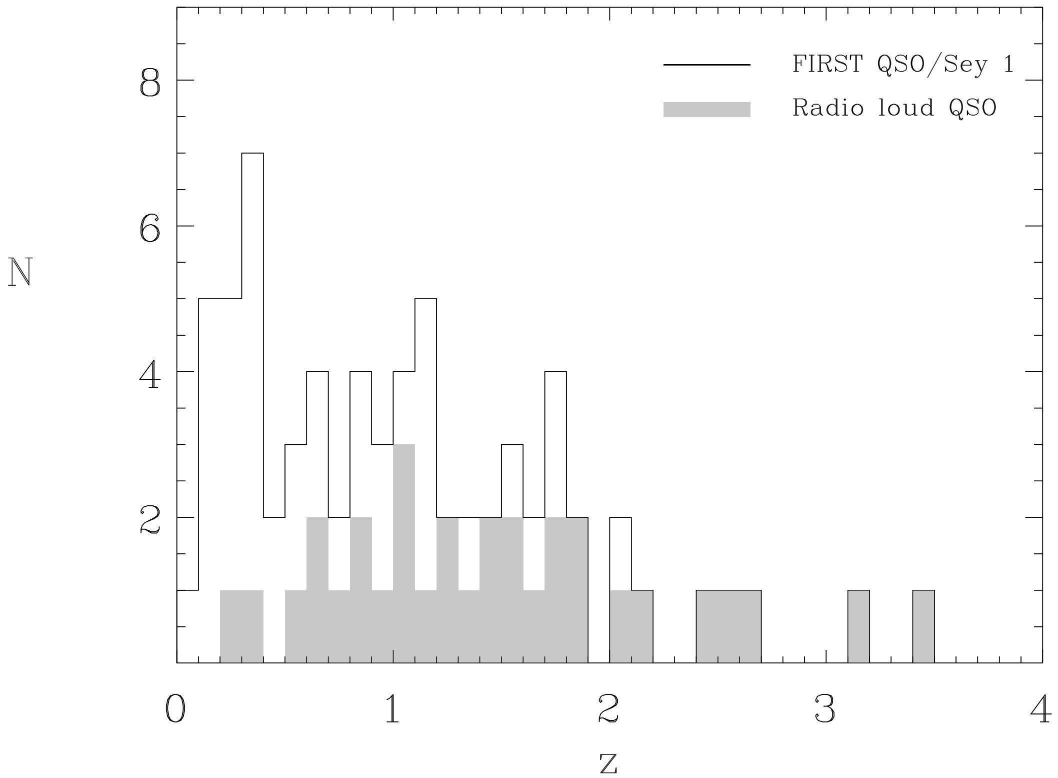

Fig. 4.— Redshift distribution of the QSO sample. Radio loud sources are shaded.

QSOs in a radio-selected sample. The fraction of radio loud objects increases from $\sim$ 15% for z$<$ 0.5 to $\sim$ 50% for 0.5 $\leq$ z $\leq$ 1.5 to $\sim$ 75% for z$>$ 1.5. The overall distribution is roughly consistent with that of the LBQS, though detailed comparisons must await better statistics when we have a larger sample.

Figure 5 shows the histogram of absolute E magnitudes derived from the APM magnitudes, adopting $\alpha_{\rm opt} = -0.5$ and the same cosmological assumptions as above. These have not been corrected for Galactic extinction or contributions from emission lines; the errors in the APM magnitudes dominate these corrections. The QSOs again suggest a bimodal distribution. The usually accepted luminosity cutoff between Seyfert 1 galaxies and QSOs is $M_B \approx -23$, which is equivalent to $M_E \sim -24$ for typical O-E of 1. The low luminosity component, containing $\sim$ 18 objects, is probably the Seyfert 1 contribution to the sample and perhaps accounts for the bimodality. All but five of the 18 were classified as stellar on both POSS plates, so deeper optical images are necessary to confirm them as Seyferts. The ELG and ALG distributions are again very similar and are plotted for comparison as a single dashed histogram. Eight of the nearest absorption line objects have either unusually bright APM magnitudes, or the APM could not assign a reliable magnitude because of complicated image structure; these are indicated by a 0. in Table 3. All of these are previously cataloged objects and a comparison with data from NED shows that the APM numbers are in error by many magnitudes. These have been excluded from the histogram and no entry for $\rm M_E$ is present in Table 3.

4. Efficiency and Completeness of the Survey

The results now allow us to evaluate the original selection criteria and formulate new improved criteria for future observations. The two primary selection criteria were the radio/optical position agreement and the APM stellar/nonstellar classification. Of the 219 candidates, 97 were classified as stellar on both plates, 29 as stellar on the E plate only, and 93 as stellar on the blue plate only. Of the 69 confirmed QSOs, the three comparable numbers are 55, 3 and 11. Clearly these numbers leave open the possibility that some QSOs are classified as nonstellar on both plates; we will return to this issue below. The reliability of the APM classifier is magnitude dependent: all 11 QSOs which are stellar on the O plate only are 18th magnitude or brighter on the O plate. Seventy-four fainter candidates are included in the initial sample of 219 because of a stellar classification from only the O plate; all but 6 of these have O-E colors redder than 2.0. Thirty of these have spectroscopic classifications and are all either ELG or ALG. In the continuation of the survey these can be eliminated by selecting objects with O-E $<$ 2.0 (see below). A color magnitude diagram of all the survey objects with redshifts and spectral classifications is shown in Figure 6.

The angular separation selection criterion turned out to be too generous. Of the 69 QSOs in the sample, 64 have separations between the radio position and optical counterpart of $< 1''\!.0$, 3 between $1''\!.0$ - $1''\!.1$, and 3 between $1''\!.1$-$2''\!.0$. The 2 QSOs with the greatest separation are extended radio sources. Of the original 219 candidates, over 25% lie outside $1''\!.1$, so a tighter matching

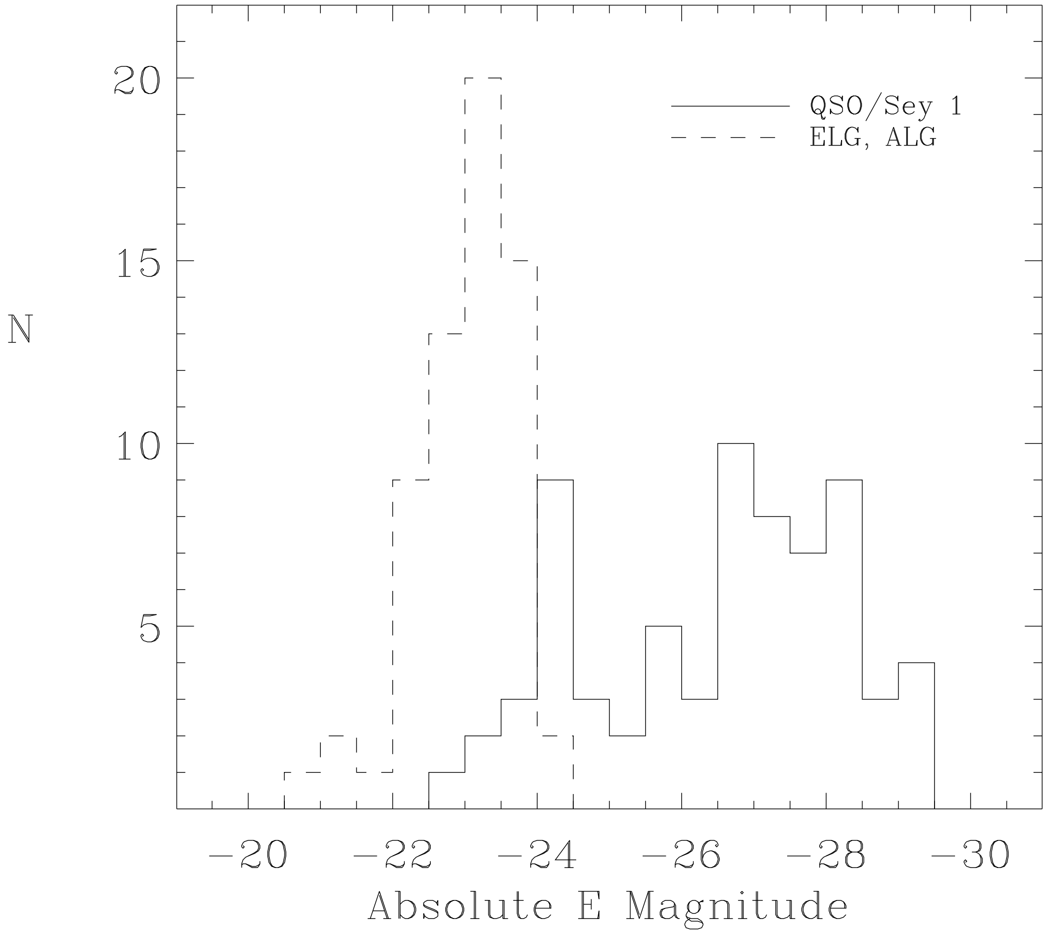

Fig. 5.— Histogram of the QSO/Seyfert 1 optical (red) absolute magnitudes (solid line); the excess in the faint tail can be explained by the lower luminosity Seyfert 1 objects present in the sample. The distributions of narrow emission line and absorption line galaxies are indistinguishable and are plotted as a single histogram (dashed line) for comparison.

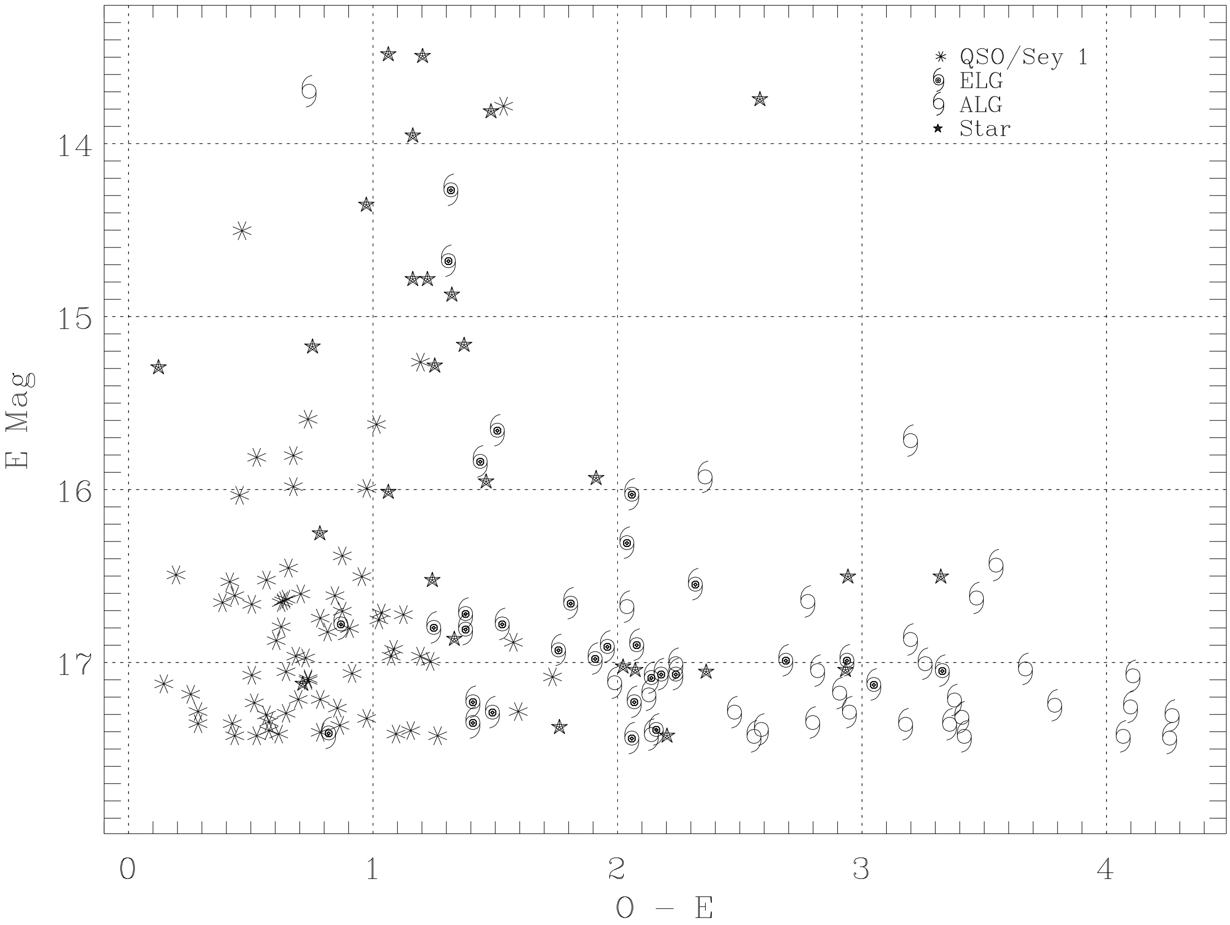

Fig. 6.— Color magnitude diagram of the entire spectroscopic sample. The reddest QSO has O-E = 1.74; emission line galaxies have colors intermediate between the QSOs and absorption line systems.

radius will eliminate many false candidates at the expense of only $\sim$ 5% of the QSOs.

Although color was not used in the original selection, the survey is not finding very red quasars: only five QSOs in the sample are redder than 1.5, the reddest with O-E = 1.74. This is perhaps because of the relatively bright magnitude limit; typical highly reddened QSOs will be much fainter in the optical (Webster et al. 1995) and will not appear in our candidate list. Imposing a color cut on our candidate sample will eliminate a sizable fraction of the non-QSO objects while sacrificing at most only a tiny number of QSOs, albeit potentially interesting ones. In the whole sample, 104 candidates out of 219 are redder than 1.75. We classified 63 of these objects spectroscopically; 34 as galaxies, 18 as ELG, 11 as Galactic stars, and none as QSOs. For an additional test of using a color cut in selecting candidates, we matched the Véron-Cetty & Véron (1996) QSO catalog against the APM catalog. Of the 380 QSOs that were within 1″ of an APM object brighter than 17.5 on the E plate, only one was redder than 2.00, confirming the utility of color as a selection criterion.

A more efficient observing program, then, would restrict candidates to those optical counterparts classified as stellar on either POSS plate, falling within a $1\rlap{.}''1$ matching radius, and with colors bluer than E-O = 2.0. If the pilot survey is typical, such a sample would be 70% QSOs and 95% complete. Only two of the 68 candidates still without spectroscopic classification in the current sample would survive the new selection criteria.

Two potential causes of incompleteness are the absence of a core radio source in a radio loud QSO, and a nonstellar classification on both POSS plates. To estimate the magnitude of these two effects, we have carried out several tests. As mentioned above, the Véron catalog of QSOs was matched with the APM catalog, selecting objects with E $<$ 17.5 and separations $< 1\rlap{.}''0$; 380 matches resulted. Of these 380 QSOs, 27 (7%) were classified as nonstellar on both POSS plates; however, only 6 ($<$ 2%) had M_B brighter than -24.3, implying that most of these are Seyfert 1 galaxies and are probably correctly classified as nonstellar.

It is more difficult to estimate the fraction of radio loud QSOs without core components. We have inspected the FIRST survey images around the positions of all the Véron QSOs in the survey area and have found one radio loud QSO (B2 1248+30) with E = 17.5 that our selection criteria missed because it has no core radio component. This suggests that few QSOs are missed because of this effect, but the test is inconclusive because other radio-selected QSO surveys may suffer from a similar incompleteness.

5. Summary and Future Plans

We have shown that the FIRST radio survey can be used in conjunction with the POSS plate material as the basis for an efficient QSO survey, highly complete for radio loud sources. With the 1994 survey data, the current FIRST catalog covers a total 1550 deg^2 and includes over 138,000 radio sources. Using our revised screening criteria, we have prepared a list of $\sim$ 400 additional

QSO candidates for spectroscopic follow-up. With this larger sample, selected in a uniform fashion and covering a large contiguous area of sky, we will begin to be able to address important questions regarding quasar radio and optical luminosity functions and their evolution, the large scale distribution of quasars, and the differences between radio loud and radio quiet objects.

We thank Chris Impey for a thorough referee's report and numerous constructive comments. The FIRST Survey is supported by grants from the National Science Foundation, NATO, the National Geographic Society, Sun Microsystems, and Columbia University. We thank Michael Strauss for taking some preliminary data in connection with this project. Part of the work reported here was done at the Institute of Geophysics and Planetary Physics, under the auspices of the U.S. Department of Energy by Lawrence Livermore National Laboratory under contract No. W-7405-Eng-48. We acknowledge extensive use of the NASA/IPAC Extragalactic Database (NED) which is operated by the Jet Propulsion Laboratory, Caltech, under contract with the National Aeronautics and Space Administration. This is Contribution Number 594 of the Columbia Astrophysics Laboratory.

Table 1. FIRST Survey Bright QSOs

R.A. (J2000)	Dec.	O	E	S_{21} Nuc (mJy)	S_{21} Tot (mJy)	z	Log(L_{21}) (erg s^{-1} Hz^{-1})	M_E
07 17 34.47	29 16 13.4	17.8	17.1	2.0	···	1.095	32.00	-26.9
07 25 26.45	29 13 41.7	18.1	17.1	1.4	···	1.34	32.00	-27.3
07 29 52.30	30 46 45.0	17.7	16.9	1.2	···	0.15	30.08	-22.9
07 44 12.04	29 59 06.7	17.9	17.5	94.9	···	1.70	34.04	-27.5
07 44 51.25	29 20 07.2	16.4	15.9	192.0	340[b]	1.18	34.04	-28.3
07 46 04.90	29 22 50.9	17.4	16.7	1.3	···	0.55	31.24	-25.8
07 51 12.35	29 19 37.3	15.0	14.6	0.9	···	0.91	31.48	-29.1
07 54 48.83	30 33 55.2	17.2	16.6	46.4	··· [c]	0.80	33.10	-26.8
07 54 58.35	29 41 54.4	17.7	17.4	410.5	···	2.106[a]	34.86	-28.1
07 59 28.30	30 10 29.0	17.4	16.7	181.9	···	1.00	33.88	-27.2
08 02 20.51	30 35 43.0	17.9	17.4	28.3	62[d]	1.64	33.49	-27.5
08 04 42.15	30 12 37.9	18.6	17.5	1245.4	···	1.446[a]	35.03	-27.2
08 09 06.22	29 12 35.6	17.2	16.5	21.7	···	1.47	33.28	-28.1
08 32 46.96	28 53 12.4	17.8	16.9	1.5	···	0.226	30.52	-23.8
08 49 02.58	30 02 34.8	17.0	16.6	0.9	···	0.660[a]	31.24	-26.4
09 12 47.81	28 54 06.5	17.9	16.8	1.0	···	0.182	30.13	-23.4
09 19 54.29	29 14 08.6	18.1	17.5	8.1	18[e]	0.72	32.25	-25.7
09 33 37.30	28 45 32.2	18.8	17.5	120.7	···	3.42	34.72	-28.9
09 37 04.05	29 37 04.9	18.0	17.4	2.4	25[f]	0.45	31.32	-24.8
09 43 11.14	29 38 04.7	18.2	17.3	0.8	···	1.77	31.98	-27.7
10 10 00.71	30 03 21.5	16.8	16.6	1.3	···	0.260[a]	30.56	-24.4
10 21 56.52	30 01 40.6	18.6	17.0	1.2	···	3.12	32.63	-29.3
10 22 30.32	30 41 05.2	17.3	16.7	921.8	···	1.316[a]	34.83	-27.7
10 26 17.46	30 36 43.0	18.1	17.0	1.6	···	0.340	30.89	-24.5
11 02 11.88	28 40 41.5	17.9	16.8	48.2	···	1.74	33.77	-28.2
11 03 13.31	30 14 42.3	18.0	17.5	108.8	166[g]	0.384[a]	32.84	-24.3
11 06 05.67	30 51 08.7	17.6	16.8	1.6	···	1.63	32.25	-28.1
11 10 40.23	30 19 09.8	18.3	17.5	22.6	87[h]	1.52	33.33	-27.3
11 22 41.47	30 35 34.9	17.4	16.7	9.8	···	1.81	33.11	-28.4
11 34 54.50	30 05 26.5	17.7	17.4	850.6	···	0.614[a]	34.13	-25.4
11 45 49.50	29 06 41.7	16.5	15.3	2.4	···	0.141	30.31	-24.3
11 52 58.77	29 30 14.8	18.6	17.5	130.8	···	1.23	33.91	-26.8
11 59 31.84	29 14 44.0	17.5	16.6	1953.1	···	0.729[a]	34.64	-26.6
12 04 37.59	28 51 25.4	17.3	16.5	5.8	···	1.14	32.50	-27.7
12 17 21.41	30 56 30.6	17.6	17.0	8.6	···	0.307[a]	31.54	-24.4
12 17 52.08	30 07 00.5	15.4	13.9	383.4	495[i]	0.237[a]	32.96	-26.9
12 21 21.94	30 10 37.1	16.7	15.7	62.8	···	0.130[a]	31.66	-23.8
12 23 13.37	29 08 24.4	17.7	17.0	1.2	···	1.12	31.78	-27.1
12 30 01.00	29 03 57.3	16.6	16.1	2.2	···	1.56	32.33	-28.7
12 32 52.75	30 15 24.0	17.9	17.2	3.5	···	0.90	32.07	-26.5
12 33 55.52	29 07 49.0	16.6	15.9	0.8	···	2.011[a]	32.13	-29.4
12 52 24.97	29 13 21.2	17.1	16.7	1.1	···	0.820[a]	31.49	-26.7
12 53 06.42	29 05 13.8	17.5	17.3	61.6	···	2.56	34.20	-28.6
13 00 28.54	28 30 10.2	17.8	17.1	197.8	···	0.648[a]	33.55	-25.9
13 14 23.15	29 10 01.8	18.3	17.4	7.2	···	1.096	32.55	-26.6
13 31 08.29	30 30 33.0	17.1	16.7	15089.3	···	0.849[a]	35.66	-26.8
13 42 54.39	28 28 05.9	18.0	17.4	68.2	180[j]	1.037[a]	33.49	-26.6
13 43 00.12	28 44 07.0	16.7	16.1	246.7	···	0.905[a]	33.93	-27.6

TABLE 1. (continued)

R.A. (J2000)	Dec.	O	E	S_{21} Nuc (mJy)	S_{21} Tot (mJy)	z	Log(L_{21}) (erg s^{-1} Hz^{-1})	M_E
13 47 37.45	30 12 52.2	16.4	15.7	15.6	···	0.12	30.98	-23.6
13 48 04.31	28 40 25.5	17.8	17.3	78.0	··· [k]	2.47	34.27	-28.4
13 48 20.89	30 20 05.6	18.0	17.3	23.3	··· [l]	1.86	33.51	-27.9
13 55 29.88	29 30 59.3	18.3	17.1	1.5	···	0.30	30.75	-24.2
14 10 36.80	29 55 51.1	17.4	17.2	3.9	···	0.57	31.72	-25.5
14 21 14.08	28 24 52.2	17.4	16.7	49.0	···	0.54	32.78	-25.8
14 55 43.42	30 03 22.5	17.5	16.7	1.5	···	0.625	31.39	-26.2
15 17 28.50	28 56 15.9	18.1	17.3	1.1	···	0.208	30.32	-23.2
15 19 36.15	28 38 27.9	17.7	16.8	1.8	···	0.270	30.75	-24.3
15 42 27.02	29 42 02.5	17.9	17.2	1.3	···	0.456	31.05	-25.0
15 42 41.14	29 34 29.2	18.0	17.4	1.5	···	1.093	31.88	-26.6
15 45 12.93	30 05 08.4	19.0	17.4	6.4	···	0.321	31.45	-24.1
15 54 29.40	30 01 19.0	17.8	16.8	41.1	···	2.69	34.06	-29.1
16 02 57.36	30 38 52.2	18.1	17.5	1.3	···	0.81	31.55	-25.9
16 03 54.16	30 02 08.9	17.7	17.2	54.1	···	2.028[a]	33.94	-28.2
16 06 48.18	29 10 48.4	18.2	17.0	1.0	···	0.33	30.65	-24.4
16 11 23.24	29 59 47.5	18.4	17.4	1.6	···	1.716	32.28	-27.6
16 14 36.83	28 39 06.0	18.9	17.2	1.9	···	0.316	30.91	-24.2
16 19 02.51	30 30 51.5	17.1	16.1	67.6	···	1.286	33.66	-28.3
16 23 07.37	30 04 06.4	17.5	16.9	1.4	···	1.168	31.89	-27.3
16 26 59.25	30 15 35.0	18.1	17.0	5.2	···	1.58	32.72	-27.8

[a]Previously known QSO

[b]0744+2920: An asymmetric double ∼ 30″ in length

[c]0754+3033: A suggestion of a weak jet ∼ 15″ in length

[d]0802+3335: An asymmetric double ∼ 60″ in extent

[e]0919+2914: A core-jet geometry ∼ 12″ in length

[f]0937+2937: May have a wide separation double ∼ 120″ in length;if so, then total flux density is 25 mJy.

[g]1103+3014: A double ∼ 60″ in extent

[h]1110+3019: An asymmetric double ∼ 45″ in length

[i]1217+3006: A core-halo morphology ∼ 50″ in diameter

[j]1342+2828: A double ∼ 40″ in extent

[k]1348+2840: A core jet morphology ∼ 15″ in length

[l]1348+3020: A core jet morphology ∼ 25″ in length; possible radio lobe along the perpendicular axis ∼ 40″ from the core

TABLE 2. Emission Line Galaxies

R.A. (J2000)	Dec.	O	E	S_{21} Nuc (mJy)	z	Log(L_{21}) (erg s^{-1} Hz^{-1})	M_E
08 25 39.72	29 11 33.8	17.3	15.7	1.4	0.092	29.70	-23.0
08 34 07.61	29 08 40.0	19.0	17.0	2.2	0.141	30.13	-22.6
08 35 47.93	28 45 11.3	13.3	12.3	12.0	0.025	29.35	-23.6
09 46 44.58	29 13 35.6	18.2	16.8	0.9	0.139	29.73	-22.8
10 22 50.59	29 11 02.8	17.4	15.9	1.5	0.134	30.05	-23.6
10 31 52.44	29 21 19.8	18.2	16.1	0.9	0.098	29.46	-22.8
11 23 51.20	30 14 40.7	17.7	16.8	0.9	0.113	29.68	-22.3
11 29 55.54	28 33 54.0	18.3	16.9	0.8	0.137	29.53	-22.7
11 49 00.27	29 58 41.2	19.8	17.1	53.0	0.158	31.60	-22.8
12 11 38.23	29 36 16.5	19.1	17.0	1.3	0.104	29.73	-22.0
12 40 35.81	30 37 23.1	19.0	17.0	1.7	0.224	30.40	-23.7
12 44 17.49	30 04 43.8	19.4	17.3	1.8	0.205	30.34	-23.2
12 51 07.68	29 19 00.6	18.3	17.5	2.8	0.206	30.52	-23.0
13 30 29.01	29 15 02.6	19.7	17.5	2.5	0.249	30.70	-23.4
13 41 32.35	30 02 44.9	19.6	17.5	0.8	0.224	30.22	-23.1
13 49 17.30	29 46 04.0	18.2	16.9	1.0[a]	0.221	30.30	-23.7
14 04 56.61	28 32 10.3	20.5	17.1	1.2	0.180	30.11	-23.1
14 28 39.56	29 34 28.9	18.7	17.3	2.1	0.153	30.08	-22.5
14 33 01.18	30 13 02.5	18.4	16.8	2.5	0.110	30.00	-22.3
14 38 22.46	30 07 03.8	20.0	17.1	3.1	0.072	29.72	-21.1
14 59 24.93	29 00 37.2	18.9	17.4	1.6	0.151	30.19	-22.4
15 00 11.40	28 53 22.2	18.6	16.7	1.6	0.125	29.79	-22.7
15 28 01.52	28 59 57.7	15.7	14.3	1.5	0.070	29.29	-23.8
15 38 41.21	29 27 32.4	16.1	14.7	1.2	0.060	29.19	-23.0
15 42 47.70	30 05 12.3	18.9	17.4	5.0	0.127	30.47	-22.0
15 48 13.46	28 53 07.8	19.4	17.1	2.0	0.180	30.44	-23.0
15 49 01.32	30 26 09.1	19.0	16.6	1.0	0.155	29.94	-23.2
16 03 25.10	29 37 56.0	18.4	16.4	1.2	0.112	29.68	-22.7
16 08 26.32	28 21 08.5	19.3	17.1	0.9	0.151	29.90	-22.7
16 08 56.72	28 47 41.8	20.3	17.2	5.2	0.243	30.94	-23.6
16 16 52.02	28 41 40.8	19.3	17.2	1.6	0.126	30.00	-22.2
16 21 25.09	29 31 49.9	18.8	17.0	1.1	0.192	30.09	-23.3

[a]not in later versions of FIRST catalog; peak flux = 0.76 mJy

TABLE 3. Absorption Line Galaxies

R.A. (J2000)	Dec.	O	E	S_{21} Nuc (mJy)	z	Log(L_{21}) (erg s^{-1} Hz^{-1})	M_E
07 36 41.52	28 41 15.0	20.1	17.5	5.2	0.185	30.76	-22.7
07 42 52.32	29 18 38.2	19.2	17.2	1.0	...	...	...
08 03 33.45	29 32 00.4	19.3	17.1	0.8	0.155	29.77	-22.8
08 50 56.85	29 12 00.6	14.5	13.8	2.6	0.027[a]	28.81	-22.3
09 00 28.14	30 46 47.2	21.5	17.3	11.2	0.268	31.45	-23.7
09 12 26.11	30 13 57.7	20.6	17.4	25.0	0.341	32.03	-24.1
09 16 41.89	30 54 55.4	0.0	9.00	1.8	0.023[a]	28.36	...
09 20 09.97	30 54 20.3	21.8	17.5	28.0	...	...	...
09 22 07.85	28 37 07.9	19.7	17.5	2.1	0.294	30.80	-23.7
09 30 16.97	29 32 24.0	11.2	11.9	5.4	0.006[a]	27.71	-20.9
09 43 09.29	29 50 18.3	21.6	17.5	4.5	0.296	31.09	-23.8
10 08 09.49	29 44 25.9	19.4	17.3	1.8	...	...	...
10 37 19.31	30 07 42.7	20.8	17.4	1.6	0.216	30.51	-23.2
10 45 24.31	29 13 08.6	13.6	12.2	4.0	0.021[a]	28.76	-23.3
10 46 23.82	30 40 07.5	18.8	16.7	1.1	0.114	29.50	-22.4
11 09 35.25	30 04 33.1	20.2	17.2	1.0	0.188:	30.13	-23.0
11 23 18.82	29 16 57.4	19.9	17.4	1.4	0.140	29.89	-22.3
11 57 09.54	28 22 00.8	20.1	17.5	27.5	...	...	...
12 18 26.52	29 48 46.5	9.1	7.5	40.1	0.013[a]	29.25	...
12 38 45.49	28 35 22.3	21.7	17.4	1.4	0.233	30.49	-23.4
13 01 49.71	30 41 33.9	20.0	17.1	1.1	0.208	30.23	-23.4
13 06 17.29	29 03 46.3	10.0	8.7	13.1	0.024[a]	29.49	...
13 08 54.24	28 11 01.5	9.9	8.3	1.2	0.020[a]	28.15	...
13 16 15.89	30 15 51.0	11.4	10.5	6.8	0.049[a]	29.74	...
13 59 24.21	29 34 08.2	20.2	17.4	15.0	0.240	31.59	-23.4
13 59 54.74	29 34 25.9	19.5	16.7	6.2	0.106	30.33	-22.3
14 00 45.82	30 04 33.5	10.2	8.3	1.9	0.027[a]	28.56	...
14 12 41.77	30 00 58.0	20.7	17.3	10.7	0.225	31.17	-23.4
14 27 22.65	29 27 07.1	20.8	17.4	1.3	0.313	30.65	-23.9
14 31 54.06	29 33 26.4	20.2	16.9	5.4	0.224	31.00	-23.7
14 32 51.07	30 03 10.0	21.1	17.3	0.8	0.220	30.09	-23.3
14 36 38.80	28 23 10.5	21.0	17.5	3.7	0.250	30.88	-23.4
15 34 34.75	29 02 53.5	20.2	16.7	10.4	0.226	31.34	-24.0
15 44 50.03	29 38 26.4	21.3	17.1	4.0	0.076	29.90	-21.2
15 47 24.51	30 11 33.7	20.3	17.4	1.2	0.240	30.46	-23.4
15 50 54.28	30 43 54.7	20.4	17.1	1.9	0.176	30.29	-23.0
15 55 12.92	29 03 29.9	18.4	16.0	25.8	0.176	31.51	-24.1
15 56 38.88	29 05 44.5	20.1	16.5	2.4	0.179	30.27	-23.7
16 06 31.68	28 49 35.3	0.0	17.1	1.3	0.227	30.27	-23.6
16 17 34.94	30 54 19.9	19.0	15.8	3.1	0.136	30.26	-23.8
16 23 42.19	28 26 24.0	20.8	17.1	2.0	0.183	30.30	-23.1

[a]Previously known galaxy

TABLE 4. Stars

R.A. (J2000)	Dec.	O	E	S_{21} Nuc (mJy)
07 18 05.62	28 43 49.4	17.2	16.1	0.8
07 21 27.24	29 28 41.6	20.1	17.1	1.9
07 32 23.41	30 28 08.7	19.5	17.1	1.0
07 52 48.48	29 19 46.1	19.2	17.1	8.5
07 57 15.87	30 10 12.9	18.0	16.0	3.6
08 07 42.51	30 43 25.4	12.8	11.4	16.2
08 39 17.07	30 29 54.4	12.4	10.7	12.1
09 06 52.13	28 55 50.2	17.9	16.6	4.8
09 38 50.60	30 51 34.9	14.7	13.6	1.3
09 47 11.82	29 14 15.6	18.3	16.9	4.8
10 01 33.44	30 52 57.7	16.6	15.4	1.1
10 20 56.13	29 41 43.2	10.9	9.6	1.1
11 16 11.68	29 07 45.9	19.9	16.6	2.5
11 19 04.94	29 51 52.9	15.5	15.4	4.7
11 24 42.02	30 36 38.5	14.8	13.6	34.1
11 35 27.07	29 38 01.0	15.4	13.9	1.2
11 54 00.52	30 39 36.9	19.7	17.5	0.9
12 04 47.02	29 32 10.7	19.3	17.5	1.0
12 16 24.20	30 20 42.5	15.2	14.0	0.8
12 36 45.93	28 35 18.9	17.1	16.3	1.2
13 20 46.38	28 58 28.7	19.6	16.6	20.8
13 20 58.44	29 05 51.4	15.4	14.4	2.3[a]
14 01 33.12	29 39 18.7	13.9	12.5	50.5
14 04 14.70	28 46 36.9	17.5	16.0	12.2
14 08 06.20	30 54 48.7	19.2	17.1	3.1
14 10 23.65	30 34 37.5	16.0	15.3	41.3
14 17 11.86	28 36 06.0	16.4	13.8	41.8
14 42 30.78	30 10 27.9	16.1	14.9	1.3
15 05 53.15	28 46 28.8	16.6	15.2	14.8
16 05 18.46	28 54 08.1	16.3	15.0	1.6
16 15 05.90	28 57 40.9	16.1	14.9	12.3

[a]Not in later versions of FIRST catalog; peak flux = 0.77 mJy

REFERENCES

Becker, R.H., White, R.L., & Helfand, D.J. 1995, ApJ, 450, 559

Becker, R.H., White, R.L., Helfand, D.J., Gregg, M.D., & McMahon, R. 1995, in *Radio Emission from the Stars and the Sun*, in press

Goldschmidt, P., Miller, L., La Franca, F., & Christiani, S. 1992, MNRAS 256, 65P

Hewett, P.C., Foltz, C.B., & Chaffee, F.H. 1995, AJ, 109, 1498

McMahon, R.G., & Irwin, M.J. 1992, in *Digitized Optical Sky Surveys*, eds. H.T. MacGillivray and E.B. Thomson, Kluwer, p. 417

Minkowski, R.L., Abell, G.O. 1963, in *Basic Astronomical Data, Volume 3 of Stars and Stellar Systems*, eds. K. Aa. Strand, University of Chicago Press, p. 481

Schneider, Donald P., van Gorkom, J.H., Schmidt, M., & Gunn, J.E. 1992, AJ, 103, 1451

Véron-Cetty, M.-P. & Véron, P. 1996, European Southern Observatory Scientific Report No. 10, *A Catalog of Quasars and Active Nuclei*, (Seventh Edition), in press

Webster, R.L., Francis, P.J., Peterson, B.A., Drinkwater, M.J., & Masci, F.J. 1995, Nature, 375, 469

Weedman, D.W. 1986, Quasar Astronomy, Cambridge University Press, Cambridge

White, R.L., Becker, R.H., Helfand, D.J., & Gregg, M.D. 1996, in preparation

This preprint was prepared with the AAS LaTeX macros v4.0.